Interfacial behaviour of sodium stearoyllactylate (SSL) as an oil-in-water pickering emulsion stabiliser

Kurukji, D.; Pichot, R.; Spyropoulos, F.; Norton, I.t.

DOI:
10.1016/j.jcis.2013.07.016

Document Version
Publisher's PDF, also known as Version of record

Citation for published version (Harvard):
Kurukji, D, Pichot, R, Spyropoulos, F & Norton, IT 2013, 'Interfacial behaviour of sodium stearoyllactylate (SSL) as an oil-in-water pickering emulsion stabiliser', *Journal of Colloid and Interface Science*, vol. 409, pp. 88-97. https://doi.org/10.1016/j.jcis.2013.07.016

Journal of Colloid and Interface Science 409 (2013) 88–97

Contents lists available at ScienceDirect

Journal of Colloid and Interface Science

www.elsevier.com/locate/jcis

Interfacial behaviour of sodium stearoyllactylate (SSL) as an oil-in-water pickering emulsion stabiliser ☆

D. Kurukji *, R. Pichot, F. Spyropoulos, I.T. Norton

Centre for Formulation Engineering, School of Chemical Engineering, University of Birmingham, Edgbaston B15 2TT, UK

ARTICLE INFO

Article history:
Received 29 April 2013
Accepted 7 July 2013
Available online 2 August 2013

Keywords:
Sodium stearoyllactylate
SSL
Pickering emulsion
DSC
Interfacial coverage
Surface coverage
Lipid particle
Melting enthalpy
Surfactant

ABSTRACT

The ability of a food ingredient, sodium stearoyllactylate (SSL), to stabilise oil-in-water (O/W) emulsions against coalescence was investigated, and closely linked to its capacity to act as a Pickering stabiliser. Results showed that emulsion stability could be achieved with a relatively low SSL concentration ($\geqslant$0.1 wt%), and cryogenic-scanning electron microscopy (cryo-SEM) visualisation of emulsion structure revealed the presence of colloidal SSL aggregates adsorbed at the oil–water interface. Surface properties of SSL could be modified by altering the size of these aggregates in water; a faster decrease in surface tension was observed when SSL dispersions were subjected to high pressure homogenisation (HPH). The rate of SSL adsorption at the sunflower oil–water interface also increased after HPH, and a higher interfacial tension (IFT) was observed with increasing SSL concentration. Differential scanning calorimetry (DSC) enabled a comparison of the thermal behaviour of SSL in aqueous dispersions with SSL-stabilised O/W emulsions. SSL melting enthalpy depended on emulsion interfacial area and the corresponding DSC data was used to determine the amount of SSL adsorbed at the oil–water interface. An idealised theoretical interfacial coverage calculation based on Pickering emulsion theory was in general agreement with the mass of SSL adsorbed as predicted by DSC.

1. Introduction

Emulsions are dispersed phase systems comprising two or more insoluble or partially soluble liquids (typically oil and water) that are used in a plethora of products, including foods, personal care products, and agrochemicals. They are thermodynamically unstable systems that revert to a lower free energy state, and given sufficient time, will completely phase separate. Thus, in order to give stabilisation for a period of time (i.e., provide kinetic stability), it is necessary to include within the formulation emulsifiers that are capable of adsorbing at the liquid/liquid interface.

Besides 'classic' emulsifiers (e.g., surfactants), particles can be used to stabilise liquid/liquid interfaces (so-called Pickering emulsions) [1]. Many particles have been researched for this purpose, including inorganics such as silica [2,3], alumina [4], and clay [5,6] through to organics such as modified starch [7], cellulose derivatives [8,9], chitin and chitosan [10,11] and carbon nanotubes [12]. However, regardless of particle type, some key factors have emerged which are deemed critical to Pickering emulsion stabilisation [13]. These include particle size and shape, extent of particle–particle interactions, and particle wettability. Smaller particles are likely to pack more efficiently than larger particles at the interface [14] but may be susceptible to desorption due to a lower interfacial desorption energy [13]. Particle–particle interactions can affect the extent of 3-dimensional particle network formation, which can serve to arrest the movement of the disperse phase droplets and/or influence adsorption at the oil–water interface [15]. Of all these factors, particle wettability is often argued to be the major determinant of emulsion stability, as this property influences how a particle will bridge the incompatible phases [16]; this is best characterised by the contact angle the particle assumes at the interface, and it has been shown that emulsion stability can be increased when the particle is preferentially wetted by the emulsion continuous phase [17].

Pickering particles in the form of fat crystals are recognised in the stabilisation of various food emulsion products, including butters, margarines, and low fat spreads [18]. In these systems the particles are organic (e.g., lipid), produced by heating a solid lipid above its melting point followed by cooling and shearing through recrystallisation to form fat crystals. One challenge in food emulsion development is to extend the range of Pickering particles that can be produced at commercial scale from approved food ingredients [19]. Approaches to achieve this will rely on using natural components such as biopolymers and lipid based materials. It is also important to produce particles in sub-micron/nanometre size range, which is a necessity for stabilisation of emulsion droplets of 0.5–10 μm [20].

* Corresponding author.
E-mail address: djk080@bham.ac.uk (D. Kurukji).

0021-9797/$ - see front matter © 2013 The Authors. Published by Elsevier Inc. All rights reserved.
http://dx.doi.org/10.1016/j.jcis.2013.07.016

Whilst a variety of approaches to the formation of Pickering particles can be envisaged, few cited in the literature rely on the natural propensity of a charged food surfactant to form ordered, crystalline aggregates in water at low concentration. One surfactant that fits this description is sodium stearoyllactylate (SSL). SSL is an anionic surfactant produced via the condensation of stearic and lactic acids that is typically used as an emulsifier and/or rheology modifier in food products (e.g., bread and cake shortenings [21,22]); it is classified as a bilayer phase (i.e., lamellar or vesicle) forming surfactant with a melting point of 40–45 °C that produces ordered structures (e.g., crystal aggregates) upon dispersion in water [23]. It has previously been stated that fatty acid tails comprising the surfactant bilayers crystallise into solid particles upon cooling below the Krafft point [21]. To-date SSL has been studied only as a low molecular weight surfactant; however, due its propensity to form ordered crystal aggregates, there is significant potential for studying it in the context of Pickering stabilisation.

Previous work with SSL in the research literature has mostly been done in the context of foam systems [22–25]. For example, Grigoriev et al. investigated the rate of adsorption at the air–water surface using SSL/Tween80 mixed emulsifiers [24]. They showed that SSL matter transfer could be increased by incorporating SSL into mixed micelles and demonstrated by Brewster angle microscopy the presence of SSL interfacial aggregates that grew and merged over time into randomly distributed 'netlike' structures. Bezeigues et al. compared a number of bilayer-forming surfactants, including SSL, with 'classic' food emulsifiers (whey protein isolate and Tween 80) [23]. These studies demonstrated that SSL was the preferred option for increasing foam stability and showed that it formed an interface with a large surface modulus. Since aggregate-laden surfaces and interfaces are more likely to possess viscoelastic rheologies [26], this data suggested that SSL could potentially provide stabilisation though a Pickering mechanism. At the time of writing only a couple [27,28] of papers were found concerning use of SSL as an O/W emulsion stabiliser; both of these studied mixtures of SSL and a polysaccharide (iota carrageenan in [27] and chitosan in [28]).

The overarching aim of this study is to investigate the behaviour of SSL at the sunflower oil–water interface and to determine whether there is potential for its use as a Pickering stabiliser. Various physical properties of SSL in aqueous media – aggregate size, stability to aggregation, and surface/interfacial tension – are studied by recrystallising SSL aggregates in water under low shear (magnetic stirring) and processing them in a high pressure homogeniser. Sunflower O/W model food emulsions are then produced in the presence of SSL aggregates and characterised by cryo-SEM, light scattering, and DSC.

2. Experimental

2.1. Materials

SSL (Grindsted® SSL P 55 Veg Kosher) was kindly donated by Danisco (Kettering, UK). The melting point of SSL was given by the manufacturer to be ~40–45 °C. The density (ρ_{SSL}) of SSL was taken from a Material and Safety Data Sheet (MSDS) as 1.063 g cm^{-1}. All water used in this study was passed through a double-distillation column equipped with a de-ionisation unit. Sunflower oil was purchased from a local supermarket. The density of sunflower oil was taken as 0.918 g cm^{-1} [29]. All materials were used directly from the manufacturer without further purification.

2.2. Methods

SSL dispersion preparation. SSL was dispersed in water at ~50–60 °C under gentle stirring. This dispersion was then cooled to room temperature (20 °C) with continued stirring. This produced a turbid dispersion containing SSL crystal aggregates. SSL concentration was calculated and reported as weight percentage, wt% (g/g). These dispersions of SSL were subjected to HPH (NS1001L Panda – GEA Niro Soavi, Italy) at 100 or 1000 bar for a single pass.

SSL particle size analysis. A few drops of the SSL dispersion after HPH was diluted into 50 g water, transferred to a polystyrene cuvette, and analysed by dynamic light scattering (DLS) (HPPS – Malvern Instruments, UK). The z-average particle diameter and polydispersity index (PDI) was recorded. Since SSL dispersions prepared by gentle stirring contained aggregates >10 μm these samples were also analysed by laser diffraction (Mastersizer HYDRO 2000SM – Malvern Instruments, UK) before HPH, immediately after HPH, and after 24 h.

Surface tension. To obtain the desired SSL concentration for analysis, a serial dilution was performed from a more concentrated 'stock' SSL solution at 20 °C. Surface tension measurements were made at 20 °C using the Wilhelmy plate method (K100 – Kruss, Germany). For critical aggregation concentration (CAC) determination, surface tension (SFT) was monitored for 30,000 s for SSL concentrations <0.05 wt% and for 6000 s at SSL concentrations >0.05 wt%. Evaporation was controlled using a plastic cover inserted over the sample. For adsorption kinetics, SFT was monitored for 6000 s before HPH and immediately after HPH at 100 bar.

Interfacial tension. Interfacial tension (IFT) was measured at 20 °C using the pendent drop method on an Easydrop goniometer (Kruss, Germany). The method used can be found in [30]; briefly, using a syringe and needle (1.8 mm diameter) containing the desired SSL dispersion, a droplet was formed in a cuvette containing sunflower oil. IFT was monitored for 5000 s at intervals using the instrumental software.

Emulsion preparation. Sunflower oil was added to the non-homogenised SSL dispersion and mixed under gentle stirring for a few minutes to allow the two phases to contact. Oil/continuous phase ratios of 20/80 and 5/95 were prepared. SSL concentration was calculated and reported as wt% (g/g) of the continuous phase. A pre-emulsion was made by subjecting this mixture to high shear mixing at 9000 rpm for 5 min (L4RT, Silverson, UK). This pre-emulsion was then subjected to HPH (NS1001L Panda – GEA Niro Soavi, Italy) at 100 bar (single pass). Emulsions were stored in the refrigerator (~3 °C) until further analysis.

Emulsion droplet size analysis. Emulsions were analysed by laser diffraction (Mastersizer HYDRO 2000SM - Malvern Instruments, UK) to determine their droplet size distributions immediately after emulsification and after two months storage at ~3 °C. Average droplet size was reported as the surface weighted mean diameter, D[3,2].

CryoSEM. Emulsion droplet structure was visualised using a Phillips XL30 FEG Cryo Scanning Electron Microscope equipped with a Gatan low temperature unit. A single drop of emulsion was placed on an analysis slide and dipped into nitrogen at −198 °C. This slide was then inserted directly into a preparation chamber at −180 °C where it was fractured and subsequently etched for 5 min at −90 °C to minimise ice formation. The surface was coated in gold and then imaged in the SEM at −130 °C.

Differential scanning calorimetry (DSC). DSC experiments were performed on a μ-DSC 3 Evo manufactured by Setaram Instruments, France. Analysis was performed on samples prepared 24 h earlier and stored under refrigeration at ~3 °C. For the dispersions and emulsions, ~700 mg was weighed using an analytical balance directly into a specialised stainless steel DSC crucible. The mass of SSL and/or sunflower oil in the crucible was back-calculated from the initial concentration of SSL in the dispersion or emulsion. All dispersions and emulsions were ramped up from 25 °C to 70 °C at 1.2 °C min^{-1} and back down to 10 °C at the same rate. Water was used as a reference. For bulk SSL, a sample mass of ~10 mg was used and the reference crucible was left empty. The bulk

material was heated from 25 °C to 70 °C at 1.2 °C min^{-1} then cooled back to 25 °C at the same rate. The melting enthalpy for SSL was obtained by calculating the area under the curve with a linear baseline using the instrument software.

3. Results and discussion

3.1. Characteristics of SSL in aqueous dispersion

Initial work centred on comparing the size and surface properties of SSL aggregates in aqueous dispersion before and after being subjected to HPH. Fig. 1a shows the effect of HPH on SSL aggregate size; except at the lowest concentration (0.1% SSL) investigated, a ten-fold increase in applied HPH pressure (from 100 to 1000 bar) afforded a significant reduction in z-average aggregate size; this reduction was attributed to the larger energy input (i.e., shear) exerted on the aggregates at the higher HPH pressure.

At 100 bar from 0.1% to 2% SSL the z-average size increased from ~210 to ~330 nm, whereas at 1000 bar it remained constant; this demonstrates that at lower pressure the aggregate size reduction achieved via HPH depended on SSL concentration and HPH energy input, with more efficient aggregate break-up occurring in the limit of lower SSL concentration. This contrasted with dispersions prepared at 1000 bar, where aggregate size reduction seemed to be independent of SSL concentration. At 100 bar and in the limit of higher SSL aggregate concentration, non-uniform aggregate break up in the homogeniser chamber became more pronounced which led to broadening of SSL aggregate size; this effect was diminished at 1000 bar as the final aggregate size reduction approached the limiting processing capability of the homogeniser. PDI, which is a measure of aggregate size distribution, decreased upon moving to a higher HPH pressure (~0.2–0.3 at 1000 bar compared to ~0.3–0.4 at 100 bar); this again can be explained by the applied pressure approaching the limit of the homogeniser processing capability and forcing more uniform aggregate break-up.

Whilst it has been shown that homogeniser processing significantly reduced SSL aggregate size, work was then undertaken to assess SSL aggregate stability post production under quiescent storage. Such information is particularly important for food formulations, where understanding of how micro-/nano-structures change over time during processing and storage is essential for engineering stability. For this purpose laser diffraction was performed to approximate average aggregate size before HPH and at time-intervals thereafter. It should be noted that laser diffraction as a particle sizing tool is preferable for aggregates >1 μm, whereas dynamic light scattering (DLS), used to obtain the data presented in Fig. 1, is more useful when the average particle size is in the submicron/nano size range, where Brownian motion dominates. In this work, z-average SSL aggregate sizes obtained from DLS measurements were found to be in general agreement with data obtained from laser diffraction; therefore, it was concluded that laser diffraction could confidently be used to determine relative changes in SSL aggregate size with time.

Fig. 2 (a = 0.5% and b = 2% SSL) shows SSL aggregate size distributions obtained by laser diffraction before HPH, immediately after, and 24 h after HPH. SSL aggregates produced solely by recrystallisation under gentle stirring were ~10–20 μm, independent of SSL

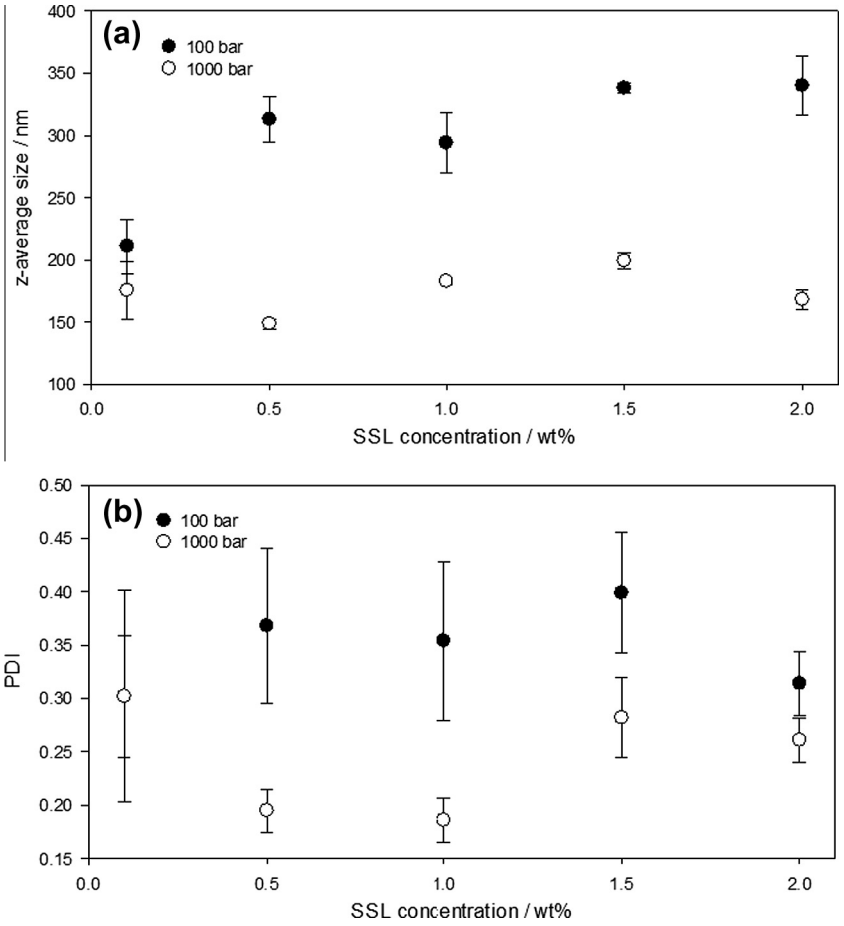

Fig. 1. Effect of HPH pressure on: (a) SSL aggregate size and (b) PDI of SSL dispersions at various SSL concentrations; two HPH pressures investigated: 100 bar (closed symbols) and 1000 bar (open symbols).

concentration. These aggregates were dispersed into colloidal aggregates with D[3,2] ~100–200 nm after HPH, in close agreement data presented in Fig. 1a. It was found that SSL re-aggregated upon storage at a rate which depended on SSL concentration. At 0.5% SSL only minor re-aggregation occurred after 24 h storage, whereas at 2% SSL nearly all aggregates had reformed to a comparable pre-HPH size. At an equivalent average aggregate size, a more concentrated SSL dispersion will have a larger aggregate surface area; it is probable that the increased re-aggregation rate was a consequence of this larger surface area, which accelerated the rate and extent of inter-aggregate collisions. Therefore, reversion to a smaller surface area, which was energetically more stable, proceeded faster at 2% SSL. It should also be expected that given sufficient time the 0.5% SSL dispersion would have reverted back to a comparable pre-HPH aggregate size, although this was not independently investigated in this study.

For both the 0.5% and 2% SSL dispersions a small peak at ~5–10 μm was observed for the sample measured immediately after HPH, although this population of aggregates was larger at 2% SSL than 0.5%. In this case, the SSL dispersion probably did not experience uniform disruptive forces within the HPH chamber, which led to broadening of the aggregate size distribution. It should also be noted that as shown previously in Fig. 1b, the HPH pressure had a significant effect on the SSL aggregate size distribution; therefore, such a bypassing effect through the HPH chamber might have been limited by increasing the homogeniser operating pressure and/or number of passes. In addition, it was also considered that re-aggregation could have begun before the initial particle size measurement had been taken; however, given the data presented in Fig. 1b, the most likely explanation is non-uniform aggregate break-up.

Static surface and interfacial tension measurements provide quantitative understanding of how surfactants diffuse and adsorb at surfaces or interfaces. Such measurements also enable quantification of surfactant properties such as critical micelle concentration (CMC) or critical aggregation concentration (CAC) if present, which, in turn, gives an understanding of how surfactants self-assemble in aqueous media. Hence, surface and interfacial tension measurements were performed to gain an understanding of these phenomena for aqueous dispersions of SSL.

First, surface tension (SFT) was measured as a function of SSL concentration, enabling approximation of the CAC (Fig. 3a). Above 0.05% SSL the 'final' SFT obtained after 6000 s was independent of SSL concentration at ~22 mN m^{-1}; this equilibrium SFT value was in agreement with reports elsewhere [23,24]. Below ~0.05%, however, the SFT data showed 'classic' adsorption behaviour in which the 'final' SFT decreased in the limit of lower SSL concentration. This demonstrated that SSL self-assembled structures (SSL bilayer aggregates) begin to form in water at ~0.05% SSL, and have a strong driving force to do so (i.e., SSL has a low monomer solubility), corroborating previous research [24].

SFT measurements were then made at SSL concentrations >CAC (0.5, 1 and 2% SSL) to investigate the kinetics of SSL surface adsorption. Given that HPH was shown to reduce SSL aggregate size by a

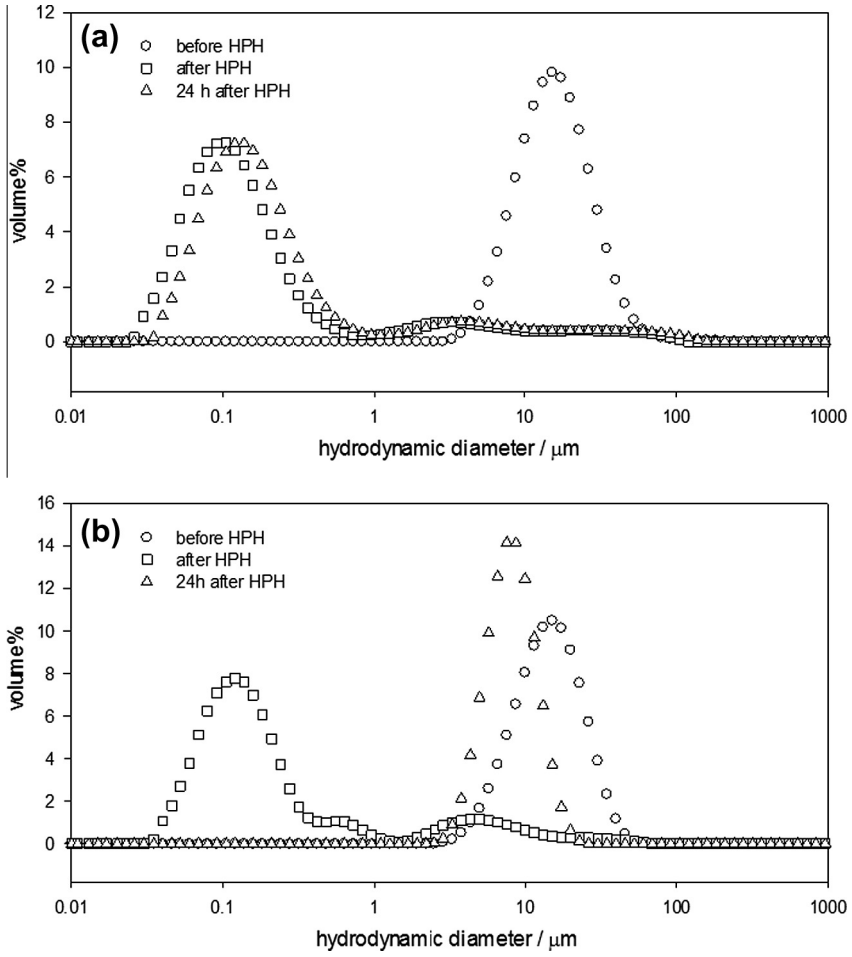

Fig. 2. Time dependency of SSL aggregate size in water. Particle size distributions measured before, just after, and 24 h after HPH (100 bar) for two SSL concentrations: (a) = 0.5% and (b) = 2%.

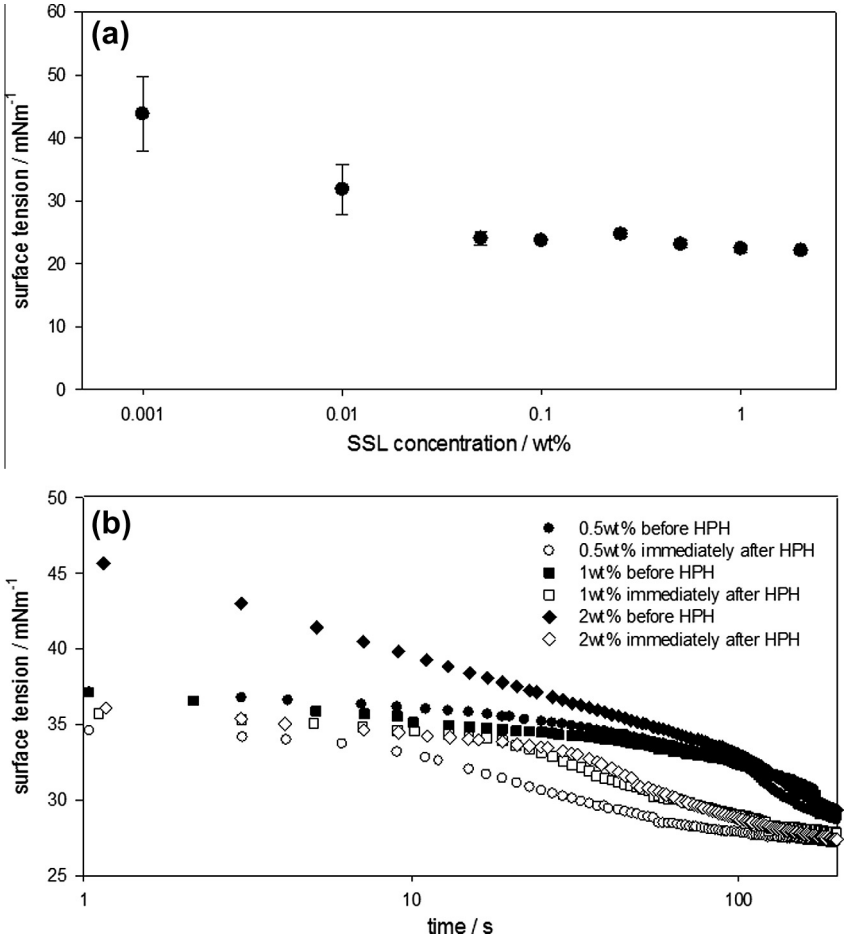

Fig. 3. Surface tension of SSL. (a) Determination of CAC for SSL dispersions before HPH; (b) dynamic surface tension for SSL dispersions before and after HPH (100 bar) for three concentrations above the CAC.

factor of ~100 (Fig. 2), it was considered that the kinetics of adsorption would also be altered due to aggregate size dependent changes in the rate of aggregate diffusion to the air–water surface.

Fig. 3b shows SFT versus time curves for SSL dispersions prepared by gentle stirring, where the average SSL aggregate size was found to be ~10–20 μm, and after HPH at 100 bar, where it was ~300 nm. Each curve showed the 'classic' decrease in surface tension followed by a levelling off to the final SFT of ~22 mN m^{-1} (note: whilst SFT was monitored up to 6000 s, the data in Fig. 3b is plotted on a log scale and shown up to 200 s to enable better visualisation of the adsorption kinetics). It can be seen that homogenised dispersions exhibited faster rates of SFT reduction than corresponding non-homogenised ones; for example, at 0.5% SSL to achieve a SFT of 32.5 mN m^{-1} required ~20–60 s for the dispersion subjected to HPH compared to ~100–200 s for the non-homogenised one; this data is consistent with the notion that colloidal SSL aggregates (~300 nm) obtained after HPH diffused more rapidly to the surface than larger SSL aggregates, which served to increase the rate of adsorption.

Another factor to consider is how the ratio of SSL monomer-to-aggregate changed with respect to total SSL concentration and as a consequence of HPH. Comparing across non-homogenised samples, the SSL monomer concentration in the system is expected to remain constant above SSL's CAC. This assumption is based on the data presented in Fig. 3a, where the CAC is considered an indication of SSL monomer solubility. On the other hand, the total SSL aggregate concentration increases with SSL added above the CAC, since additional SSL added beyond this point goes into forming SSL aggregates. Comparing across the homogenised dispersions, however, the assumption that the monomer concentration remained constant is not necessarily valid since any dynamic equilibrium between SSL monomer and aggregate, if present, could have been perturbed by HPH. Therefore, in this case, it is not possible to demonstrate whether an increase in the rate of surface adsorption is due solely to faster SSL aggregate diffusion, or whether a higher effective SSL monomer concentration additionally contributed to the rate increase. Whilst it has previously been stated that intensive heating or stirring can only slightly enhance the rate of SSL surface adsorption [24], the data here shows that HPH processing and its influence on SSL aggregate size and/or monomer concentration, can significantly influence adsorption kinetics.

Interfacial tension (IFT) measurements using sunflower oil were then performed on non-homogenised and homogenised SSL dispersions (SSL concentrations >CAC). These measurements were done to compare against SFT data presented previously and to gain information about the behaviour of SSL at the sunflower oil–water interface. Fig. 4 shows IFT curves for 0.5%, 1% and 2% SSL before and after HPH at 100 bar. In agreement with the surface tension data, SSL adsorption was faster after SSL aggregate break-up via HPH.

Interestingly, IFT readings measured after 5000 s (near equilibrium) were significantly different despite being performed at SSL concentrations >CAC; this contrasted with the SFT data where final SFT values of ~22 mN m^{-1} were obtained, independent of SSL concentration and irrespective of whether the SSL dispersion had been subjected to HPH. For example, comparing across the non-homog-

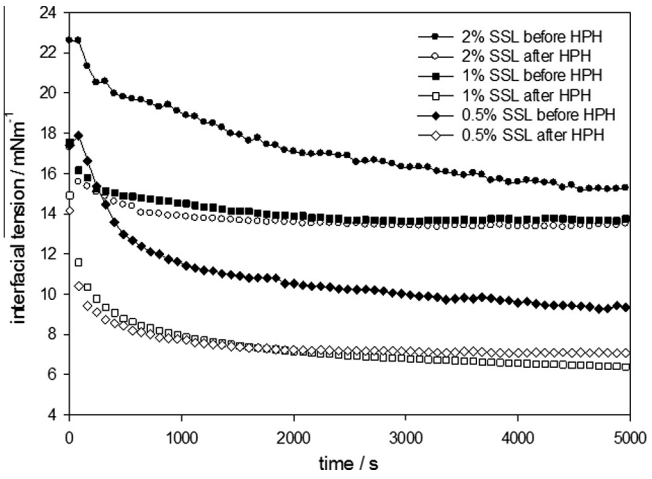

Fig. 4. Interfacial tension of SSL before (full symbols) and after HPH at 100 bar (open symbols) for three SSL concentrations above the CAC (0.5%, 1%, and 2%).

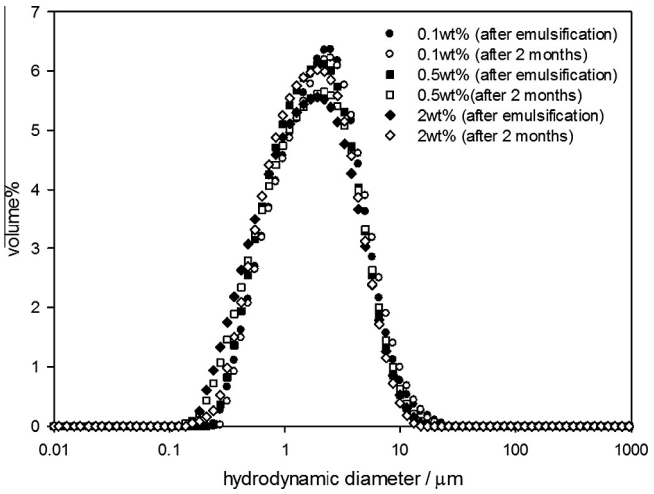

Fig. 5. O/W emulsion droplet size distributions at 0.1%, 0.5% and 2% SSL measured after emulsification (full symbols) and after two months storage (open symbols).

enised SSL dispersions, IFT after 5000 s was reduced from ~16 mN m^{-1} at 2% SSL to ~10 mN m^{-1} at 0.5% SSL. This counterintuitive result suggests that SSL aggregate concentration directly influences equilibrium interfacial composition; as SSL concentration is raised above the CAC it is probable the interfacial composition is increasingly dominated by SSL aggregates rather than monomer. This is also apparent when comparing the SSL dispersion at 1% before and after HPH. Whilst a faster reduction in IFT can be explained by a reduction in aggregate size and/or viscosity caused by HPH, the difference in IFT after 5000 s must have been a consequence of a difference in the composition of the interface.

3.2. Sunflower oil-in-water emulsion formation in the presence of SSL

To investigate emulsification in the sole presence of SSL as a stabiliser, model food O/W emulsions were prepared with sunflower oil as the dispersed phase. After preliminary studies a HPH pressure of 100 bar was chosen to obtain a D[3,2] ~ 2 μm. This is an important consideration since it has previously been stated that for Pickering emulsion formation the average particle size must be at least an order of magnitude smaller than the average emulsion droplet size [20]. Furthermore, formation of 'micron-sized' droplets facilitated the visualisation of the droplet interface by cryo-SEM (presented later), which is increasingly difficult in the limit of sub-micron or nano-sized droplets.

Droplet size distributions were measured by laser diffraction immediately after emulsification and after two months quiescent storage in a refrigerator at ~3 °C (Fig. 5). It can be seen that the D[3,2] after HPH was ~2 μm, and the final size did not depend on SSL concentration. Droplet size distributions were mono-modal, both after emulsion formation and after two months storage. This demonstrated that a relatively low SSL concentration conferred droplet stability to coalescence.

From the droplet size data presented in Fig. 5 it was not possible to demonstrate whether or not colloidal SSL aggregates produced during HPH remained intact upon adsorption at the oil–water interface, or whether they released SSL in monomeric form. IFT results presented in section 3.1 suggested significant differences in interfacial composition, depending on SSL aggregate concentration. Moreover, it has previously been suggested that for bilayer forming surfactants such as SSL the packing conditions in aqueous dispersion are closely related to those found in condensed liquid–liquid films [21]. If this is true, interfacial rheological properties such as the dilational modulus would be expected to large in comparison to typical low molecular weight surfactant interfacial layers. Indeed, previous dynamic rheology experiments [22] at the air–water surface have shown that a 0.1% SSL aqueous dispersion has a dilational modulus in excess of 1700 mN m^{-1}. However, to-date, interfacial rheology experiments with SSL at an oil–water interface have yet to be reported.

In order to shed light on how SSL behaved at the oil–water interface, a microscopy technique, cryo-SEM, was performed to visualise the droplet interface. This technique has previously found to be invaluable for visualising emulsion-based systems [31,32], and in particular, interfacial structure. Fig. 6 (a = 0.1% and b = 2% SSL) displays micrographs of emulsion droplets stabilised solely by SSL; the presence of SSL colloidal aggregates (~100–200 nm) adsorbed at the oil–water interface can clearly be visualised. There appeared to be concentration-dependent differences in interfacial structure: at 2% SSL the aggregates were spherical and appeared to fully cover the interface, whereas at 0.1% the interface seemed to be only sparsely covered with irregularly shaped aggregates. Hence, these micrographs confirm that SSL nano-crystal aggregates adsorb at the sunflower oil–water interface, resulting in a Pickering mechanism of stabilisation.

It should also be mentioned that whilst IFT varied with SSL concentration, the average droplet sizes obtained after HPH were similar. This is surprising since a lower IFT usually favours droplet break-up during emulsification. However, the final average size after processing ultimately depends on a combination of 'process-controlled' (e.g., hydrodynamics, time) and 'formulation-controlled' (e.g., viscosity, emulsifier) factors. IFT measurements performed in this study (Section 3.1) only provide information about SSL adsorption under static conditions, which does not necessarily correlate with adsorption rates under dynamic conditions of emulsion formation, where the hydrodynamics are vastly different. It appears in this system that factors aside from SSL concentration strongly influence the final droplet size obtained after processing.

3.3. DSC analysis

Since SSL is a crystalline solid at ambient temperature, DSC measurements were performed to gain information about its thermal behaviour in bulk, recrystallised dispersion, and O/W emulsified forms. DSC heating and cooling traces are shown in Fig. 7 (a = bulk SSL, b = 2% SSL dispersion, and c = 2% SSL-stabilised O/W emulsion at 20% oil mass fraction). Endothermic transitions (e.g.,

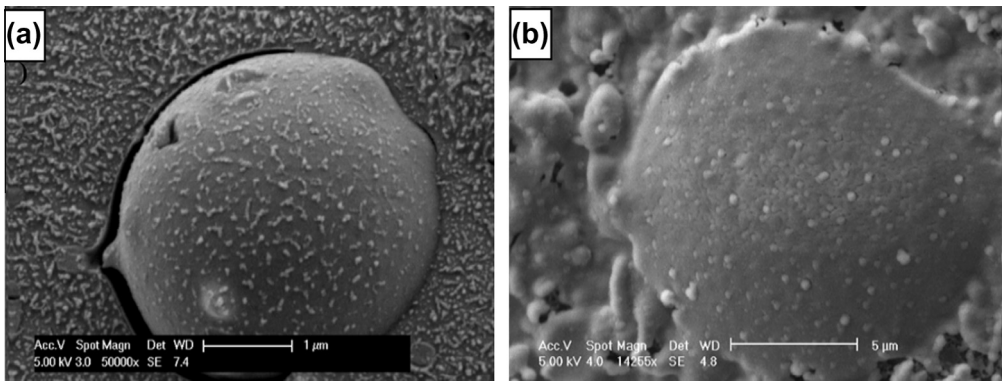

Fig. 6. Cryo-SEM micrographs of emulsion oil droplets stabilised with (a) 0.1% and (b) 2% SSL.

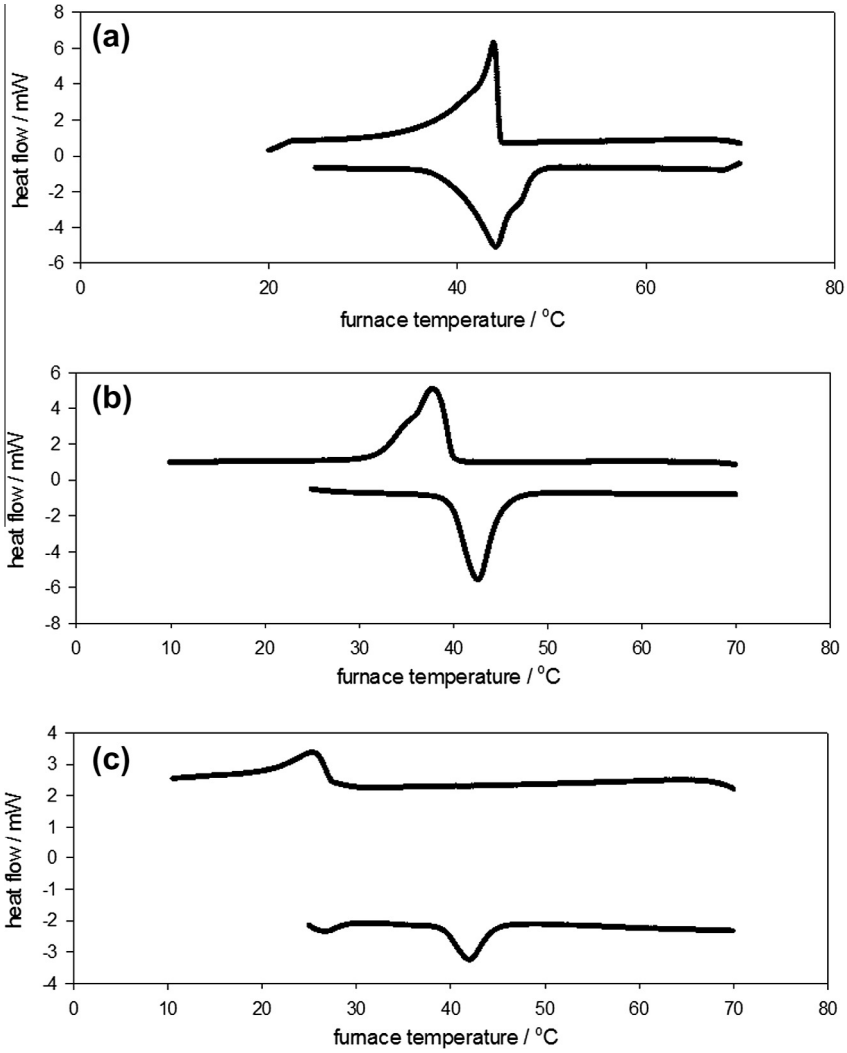

Fig. 7. DSC heating and cooling traces for (a) bulk SSL, (b) aqueous SSL dispersion (2% SSL), and (c) O/W emulsion (2% SSL, 20% sunflower oil).

melting) have negative heat flows whereas exothermic transitions (e.g., recrystallisation) have positive heat flows.

The heating curve for solid SSL in bulk form possessed an endotherm with a peak temperature of 44.2 ± 0.78 °C, indicative of SSL melting, followed by a recrystallisation exothermic transition upon cooling with a peak temperature of 43.2 ± 0.96 °C (Table 1). The melting transition was relatively broad, probably indicative of impurities in commercial SSL. As expected for bulk lipids in general, recrystallisation of SSL occurred at a comparable temperature to its melting.

DSC curves for SSL dispersions demonstrated a number of differences to SSL in bulk form. A peak melting transition of the dispersion was observed at an equivalent temperature, 43.0 ± 0.24 °C, to bulk SSL but with a slightly lower recrystallisation

Table 1
Peak SSL melting and recrystallisation temperatures. Dispersions and O/W emulsions contained 2 % SSL. Errors are expressed as one standard deviation of triplicate measurements.

	Peak melting temperature (°C)	Peak crystallisation temperature (°C)
Bulk SSL	44.2 ± 0.78	43.2 ± 0.96
SSL dispersion	43.0 ± 0.24	38.0 ± 1.0
Emulsion (5 wt% oil)	43.3 ± 0.81	34.8 ± 3.8
Emulsion (20% oil)	42.0 ± 0.89	25.0 ± 1.7

temperature: 38.0 ± 1.0 °C. This necessity for supercooling moving from bulk to aqueous dispersed lipid has been reported numerous times before [33–35] and is attributed to the retardation of nucleation due to dispersion of a lipid into aqueous aggregates. An onset delay of crystallisation of only ~5 °C for SSL differed to reported data for other lipid systems that often show delays in excess of 20 °C [36]. However, a recent study [36] with another anionic lipid based emulsifier (glyceryl stearylcitrate) similarly showed this minimal requirement for supercooling; this was attributed to the orientation of the fatty chains and esterified citric acid head groups, which were argued to act as a template for heterogeneous nucleation. It is probable that a similar effect occurred for these charged SSL bilayer aggregates, where the lactylate groups were exposed to the aqueous phase and the stearoyl fatty tails inwards. This mechanism would explain the minimal requirement for supercooling in this system.

As a general rule, aqueous dispersed lipid aggregates usually exhibit lower and broader melting points than corresponding bulk lipids [33–36]. It is known that lipid crystal aggregate size has an effect on the magnitude of the melting point reduction [33,35,36]. In the limit of their smaller size, crystal aggregates possess larger surface area-to-volume ratios and hence higher chemical potentials; therefore, they typically melt at lower temperatures [33]. SSL dispersions in this work were analysed by DSC without being subjected to HPH and had an average aggregate size of ~10–20 μm. One explanation for the negligible reduction in melting temperature could have been a consequence of their large size relative to nano-sized aggregate analysed in other studies.

Thermal profiles for the SSL-stabilised O/W emulsions also demonstrated differences to bulk SSL and the dispersions. Whilst the peak SSL melting temperatures for the O/W emulsions were comparable to bulk and aqueous dispersed SSL, a progressive reduction in peak recrystallisation temperature was observed with increasing sunflower oil mass fraction (see Table 1); this was attributed to a reduction in SSL solubility with increased sunflower oil dispersed phase interfacial area. For a fixed SSL concentration, a greater interfacial area at 20% oil resulted in a greater amount of SSL in adsorbed form; this served to reduce overall SSL solubility and increase the supercooling requirement.

It was also observed that at an equivalent SSL concentration, the SSL-stabilised O/W emulsion had a significantly lower SSL melting enthalpy than the corresponding SSL aqueous dispersion. Therefore, a series of aqueous dispersions and O/W emulsions (at two sunflower oil mass fractions) were prepared with varying SSL. Melting enthalpy from DSC was then plotted against the mass of SSL present in dispersion or emulsion. Since a known mass (~700 mg) of dispersion or emulsion was added to the DSC crucible, the total mass of SSL (and sunflower oil for the emulsions) contained within them could be calculated accurately.

For SSL in aqueous dispersion, an increase in the mass of SSL resulted in an increase in melting enthalpy, and the relationship was linear and passed through the origin (Fig. 8); a linear trend was observed for O/W emulsions prepared at different oil mass fractions, although all of the O/W emulsions demonstrated lower SSL melting

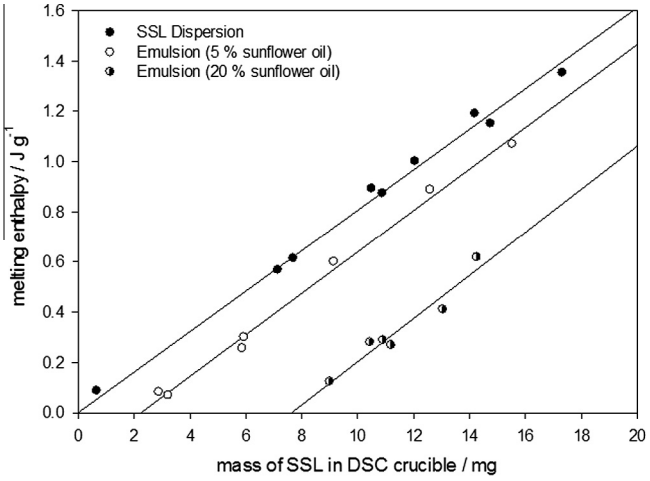

Fig. 8. Melting enthalpy versus mass of SSL present.

enthalpies. Moreover, the melting enthalpy reduction for the O/W emulsions also depended on the sunflower oil mass fraction, with a larger reduction observed at 20% than 5% sunflower oil. Whilst the SSL dispersion regression line passed through the origin, as expected due to the mass of melting material (i.e., SSL) present equating to zero at this point, the O/W emulsion regression lines intercepted at defined masses of SSL: 2.3 mg and 7.7 mg for those prepared at 5% and 20% oil mass fractions, respectively.

The main structural difference between an SSL dispersion and O/W emulsion is the presence of an oil–water interface in the latter. Therefore, in order to rationalise the data in Fig. 8, we consider the role of the O/W interface: we hypothesise that the magnitude of the regression line intercepts for the O/W emulsions (2.3 mg SSL for 5% sunflower oil and 7.7 mg for 20% sunflower oil) quantifies the mass of SSL adsorbed at the oil/water interface. This is consistent with the data in Fig. 8, since a larger intercept SSL mass value is observed at 20% than 5% sunflower oil, which implies a greater amount of adsorbed SSL. An equation was derived using Pickering emulsion theory to approximate the mass of SSL adsorbed at the O/W interface.

The total mass of SSL aggregates adsorbed at the oil–water interface, M_{int}, can be expressed as:

$$M_{int} = n_{p,int} \times m_{\rho,SSL} \tag{1}$$

where $n_{p,int}$ is the total number of SSL aggregates adsorbed and $m_{\rho,SSL}$ is the average mass of an SSL aggregate.The mass of a spherical SSL aggregate, $m_{p,SSL}$, is given by:

$$m_{\rho,SSL} = \frac{4\pi r_p^3}{3} \times \rho_{SSL} \tag{2}$$

where r_p is the aggregate radius and ρ_{SSL} is the density of SSL (1.063 g cm^{-3}).The total number of SSL aggregates adsorbed at the oil–water interface is expressed by the following:

$$n_{p,int} = n_d \varphi \frac{SA_d}{SA_p} \tag{3}$$

$$n_{p,int} = \frac{\varphi m_{oil}}{4/3\pi\rho_{oil} r_d r_p^2} \tag{4}$$

where SA_d is the surface area of a droplet of radius r_d, SA_p is the surface area of an SSL aggregate of radius r_p, φ is the interfacial coverage of SSL aggregates at the O/W interface, n_d is the total number of sunflower oil droplets, m_{oil} is the mass of sunflower oil present in the emulsion, and ρ_{oil} is the density of sunflower oil

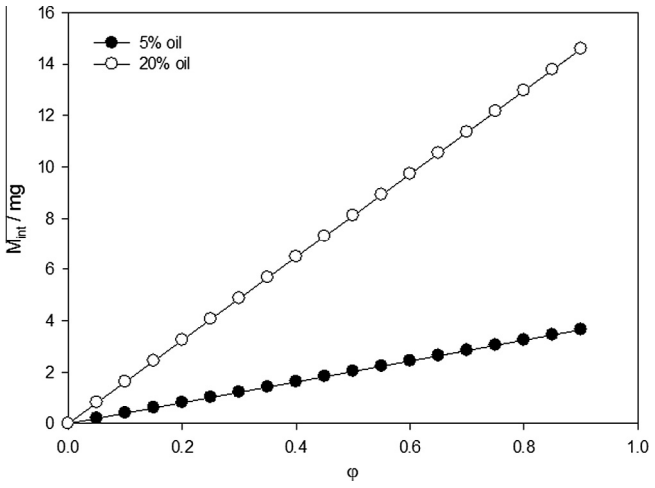

Fig. 9. Plot of M_{int} versus packing fraction using (Eq. (5)).

(0.918 g cm^{-1}).Finally, substituting Eqs. (2) and (4) into (1) and simplifying gives (5):

$$M_{int} = \frac{r_p \varphi m_{oil} \rho_{SSL}}{r_d \rho_{oil}} \quad (5)$$

A number of two-dimensional particle packing arrangements are feasible at a droplet interface, including hexagonal, triangular, and square. In the case of hexagonal, which is the most efficient packing arrangement, φ can adopt any value between zero and ~0.9, where the upper limit is the approximate limiting packing density for uniform spheres on a two-dimensional plane, i.e., $\varphi = \pi/(2\sqrt{3}) = 0.907$ [20]. In this study, Eq. (5) was derived and used under the following assumptions: (1) SSL functions as Pickering stabiliser; (2) SSL aggregates form a 90° contact angle with respect to both the oil and continuous phases; (3) the aggregates adsorb as spherical, rigid entities; and (4) there is monolayer coverage. For this analysis, r_p was fixed at 100 nm, chosen on the basis of the SSL aggregate size data (see Fig. 1a) and cryo-SEM micrographs (see Fig. 6). r_d was taken as 1000 nm, one-half of the D[3,2] from laser diffraction (see Fig 5).

A plot of M_{int} versus φ at these fixed r_p and r_d values approximates SSL interfacial coverage (Fig. 9). Eq. (5) shows good agreement with the O/W emulsion intercept DSC data presented in Fig. 8. At both 5% and 20% oil, Eq. (5) predicts the corresponding DSC intercepts (2.1 mg SSL at 5% oil and 7.7 mg at 20% oil) at $\varphi \sim 0.5$. It should be noted that this calculation depends on assumptions described previously that introduces a degree of error into the interfacial coverage approximation. Ultimately this analysis supports the notion of a Pickering mechanism of stabilisation and shows that DSC can be a powerful tool for quantifying interfacial coverage in this system.

4. Conclusions

The novelty of the route to Pickering particle formation in this work stems from the natural propensity of SSL to form ordered, stable bilayer aggregates at low concentration in aqueous media. SFT measurements demonstrate this driving force for SSL bilayer formation at low concentration and show that SSL adsorption kinetics can be significantly modified by altering the size of SSL aggregates in water via HPH. IFT studies demonstrated SSL concentration-dependent differences in interfacial composition, resulting from aggregate adsorption at the interface. O/W emulsions prepared solely with SSL demonstrated excellent stability to coalescence, and this could be achieved using a relatively low SSL concentration. DSC was shown to be an invaluable tool for elucidating differences between the thermal behaviour of SSL in aqueous dispersion with that in O/W emulsion, and for this system, it enabled quantitative differences to be ascertained between non-adsorbed and adsorbed SSL. Theoretical calculations agreed with the DSC data and hence provided additional support for the Pickering mechanism of stabilisation. This evidence was strengthened by cryo-SEM visualisation of colloidal SSL aggregates adsorbed at the O/W interface.

Ultimately, this paper demonstrates a novel approach to the formation of food-grade Pickering particles. Typical food-grade particle syntheses often require significant and complex processing before they can be useful as Pickering stabilisers [37–39]; this can limit their viability from both a regulation and cost viewpoint. In this case, SSL Pickering particles are produced from a food-grade material in a way that minimises the need for extensive particle processing. Furthermore, this is the first systematic study investigating the behaviour of SSL as the sole stabiliser at an oil–water interface, and where a Pickering mechanism is proposed. Additional work would benefit from understanding how the ratio of monomer to aggregate in the system impacts resulting interfacial structure. For example, it may be possible to tune interfacial structure from monomer- to aggregate-rich simply by increasing/decreasing SSL concentration. Previous work at the air–water surface has alluded to SSL aggregate spreading at the air–water surface to create a monomer-laden interface [24]; however, evidence in this work points towards the potential for adsorption of discrete SSL aggregates. It would also be interesting to see how different oils affect this adsorption behaviour, as this would potentially influence aggregate wetting. We have shown for the first time that DSC can be used to quantify interfacial coverage through SSL's reduction in melting enthalpy upon adsorption; additional work would benefit from further calorimetric and structural investigations to verify why SSL crystallinity decreases through its adsorption at the O/W interface. Moreover, it would be worthwhile to investigate whether interfacial coverage of other surface active compounds could be quantified using DSC, since this may have useful applications in modelling, as well as in diagnostics.

Acknowledgments

The authors acknowledge the Technology Strategy Board (TSB), the Engineering and Physical Sciences Research Council (EPSRC) and Syngenta for provision of funding to complete this work. The authors would like to thank Phil Taylor and Patrick Mulqueen for fruitful discussions.

References

[1] S.U. Pickering, Journal of the Chemical Society 91 (1907) 2001–2021.
[2] J. Frelichowska, M.A. Bolzinger, Y. Chevalier, Colloids and Surfaces a-Physicochemical and Engineering Aspects 343 (1–3) (2009) 70–74.
[3] B.P. Binks, S.O. Lumsdon, Physical Chemistry Chemical Physics 1 (12) (1999) 3007–3016.
[4] J. Chen et al., Colloids and Surfaces a-Physicochemical and Engineering Aspects 382 (1–3) (2011) 238–245.
[5] S. Guillot et al., Journal of Colloid and Interface Science 333 (2) (2009) 563–569.
[6] S.A.F. Bon, P.J. Colver, Langmuir 23 (16) (2007) 8316–8322.
[7] B.S. Murray et al., Food Hydrocolloids 25 (4) (2011) 627–638.
[8] B.L. Holt et al., Journal of Materials Chemistry 20 (45) (2010) 10058–10070.
[9] M. Kargar et al., Journal of Colloid and Interface Science 366 (1) (2012) 209–215.
[10] M.V. Tzoumaki et al., Food Hydrocolloids 25 (6) (2011) 1521–1529.
[11] Z.J. Wei et al., Polymer 53 (6) (2012) 1229–1235.
[12] M. Shen, D.E. Resasco, Langmuir 25 (18) (2009) 10843–10851.
[13] R. Aveyard, J.H. Clint, T.S. Horozov, Physical Chemistry Chemical Physics 5 (11) (2003) 2398–2409.
[14] D. Rousseau, Food Research International 33 (1) (2000) 3–14.
[15] B.P. Binks, J.A. Rodrigues, Langmuir 23 (14) (2007) 7436–7439.
[16] B.P. Binks, J.H. Clint, Langmuir 18 (4) (2002) 1270–1273.
[17] B.P. Binks, Current Opinion in Colloid & Interface Science 7 (1–2) (2002) 21–41.

[18] I. Norton, P. Fryer, S. Moore, Aiche Journal 52 (5) (2006) 1632–1640.
[19] V.J. Morris, Trends in Biotechnology 29 (10) (2011) 509–516.
[20] E. Dickinson, Trends in Food Science & Technology 24 (1) (2012) 4–12.
[21] N. Krog, Cereal Chemistry 58 (3) (1981) 158–164.
[22] J.J. Kokelaar, J.A. Garritsen, A. Prins, Colloids and Surfaces a-Physicochemical and Engineering Aspects 95 (1) (1995) 69–77.
[23] J.B. Bezeigues et al., Colloids and Surfaces a-Physicochemical and Engineering Aspects 331 (1–2) (2008) 56–62.
[24] D.O. Grigoriev et al., Colloids and Surfaces a-Physicochemical and Engineering Aspects 301 (1–3) (2007) 158–165.
[25] M.G. Semenova et al., Colloids and Surfaces B – Biointerfaces 31 (1–4) (2003) 47–54.
[26] D.E. Tambe, M.M. Sharma, Advances in Colloid and Interface Science 52 (1994) 1–63.
[27] M. Flores et al., Meat Science 76 (1) (2007) 9–18.
[28] K.G. Zinoviadou et al., Procedia Food Science 1 (2011) 57–61.
[29] M.A. Grompone, Bailey's Industrial Oil and Fat Products, in: S. Fereidoon (Ed.), sixth ed., vol. 1–6, 2005.
[30] R. Pichot, F. Spyropoulos, I.T. Norton, Journal of Colloid and Interface Science 377 (1) (2012) 396–405.
[31] R. Pichot, F. Spyropoulos, I.T. Norton, Journal of Colloid and Interface Science 352 (1) (2010) 128–135.
[32] S. Frasch-Melnik, F. Spyropoulos, I.T. Norton, Journal of Colloid and Interface Science 350 (1) (2010) 178–185.
[33] B. Siekmann, K. Westesen, Colloids and Surfaces B: Biointerfaces 3 (3) (1994) 159–175.
[34] M. Higami et al., Journal of the American Oil Chemists' Society 80 (8) (2003) 731–739.
[35] H. Bunjes, M.H.J. Koch, K. Westesen, Langmuir 16 (12) (2000) 5234–5241.
[36] R. Gupta, D. Rousseau, Food & Function 3 (3) (2012) 302–311.
[37] A. Timgren et al., Starch particles for food based Pickering emulsions, in: 11th International Congress on Engineering and Food (Icef11), vol. 1, 2011, p. 95–103.
[38] R. Santipanichwong et al., Journal of Food Science 73 (6) (2008) N23–N30.
[39] J.W.J. de Folter, M.W.M. van Ruijven, K.P. Velikov, Soft Matter 8 (25) (2012) 6807–6815.